

# Meta-Learning Transferable Parameterized Skills

Haotian Fu, Shangqun Yu, Saket Tiwari, George Konidaris, Michael Littman

Department of Computer Science, Brown University  
Providence, RI

## Abstract

We propose a novel parameterized skill-learning algorithm that aims to learn transferable parameterized skills and synthesize them into a new action space that supports efficient learning in long-horizon tasks. We first propose novel learning objectives—trajectory-centric diversity and smoothness—that allow an agent to meta-learn reusable parameterized skills. Our agent can use these learned skills to construct a temporally-extended parameterized-action Markov decision process, for which we propose a hierarchical actor-critic algorithm that aims to efficiently learn a high-level control policy with the learned skills. We empirically demonstrate that the proposed algorithms enable an agent to solve a complicated long-horizon obstacle-course environment<sup>1</sup>.

## 1 Introduction

Deep reinforcement learning (RL) has been successful in various continuous control tasks [1; 2]. However, RL algorithms typically struggle to complete long-horizon tasks, like the obstacle course shown in Figure 1. Hierarchical RL [3] methods propose to decompose the long-horizon problem into several easier subtasks and thus accelerate learning; the idea is that the agent can learn skills for solving each subtask and then reuse them to solve more complex tasks. A large body of previous work learns discrete skills and then learns when to execute those **discrete** skills to solve higher-level tasks. However, such skills are not flexible enough for use in realistic tasks: in many cases, the policy necessary to solve a subtask varies across tasks. A real world of this idea is a robot picking and placing a cup to make coffee. To execute the behavior, it must know the specific position, in 3D coordinates ( $x, y, z$ ), to place the cup; the specific choice of coordinates may vary from task to task. We address this challenge by learning *parameterized skills* [4] that augment a discrete skill with continuous parameters; the parameters make the skills more likely to be reusable in new tasks because they are flexible enough to be applied in diverse situations.

Adopting this approach, the first question that arises is how to learn a transferable parameterized skill from a set of similar tasks. We aim to let the agent associate a continuous latent value to a concrete task and learn to modify its behavior in response to these values. Meta-reinforcement learning (meta-RL) algorithms [5; 6] provide a way to learn a generalizable policy from a set of similar tasks

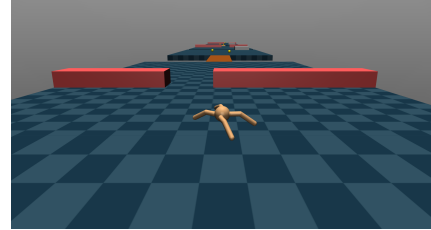


Figure 1: An obstacle course faced by a robot ant. The agent must solve several different categories of challenges (passing through a door, crossing a bridge, gathering coins, and pushing a box to form a bridge) to reach the goal. The task requires over 5000 environmental steps to successfully complete.

<sup>1</sup>A video of the learned policy can be found at <https://youtu.be/eHPbRuroKGM>.

so that the agent can quickly adapt to a new task within a few interactions with the environment. The policies learned by meta-RL methods can perform quite well on a single task drawn from the distribution over similar tasks. However, to synthesize such policies into a new action space and efficiently learn a high-level policy that composites different sub-policies to complete tasks with a much longer horizon, we propose additional trajectory-centric diversity and smoothness training objectives that lead to a structured continuous representation space of the learned skills.

After obtaining the parameterized skills, a remaining issue is how to efficiently learn a high-level control policy using these fixed skills. Some previous work has focused on RL problems where such a parameterized/discrete-continuous-hybrid action space is given by the environment [7; 8]. In contrast, our parameterized action space is learned, so the new action space can be quite noisy as each high-level task involves a large number of interactions with the low-level policy, which is also learned. Compared with the state-of-the-art algorithm for parameterized action spaces, HyAR [9], which proposes to plan in a latent embedding space of the original parameterized actions, as well as P-DQN [10; 8], which may suffer from scalability and redundancy issues, we propose a simpler and more effective algorithm able to efficiently learn a high-level control policy with the learned parameterized skills.

We validate our approach on a long-horizon ant obstacle course task, while also separately showing the superiority of the two parts of our algorithm independently by comparing with previous meta-RL and parameterized action space RL algorithms. After learning the parameterized skills, our high-level agent only needs 15 high-level steps to complete the aforementioned 5000-step problem.

## 2 Background

We adopt the standard Markov Decision Process (MDP) setting, where  $S$  is the state space,  $A$  is the action space,  $T$  is the transition function,  $R$  denotes the reward function and  $\gamma$  is the discount factor. A common way to learn temporal abstraction over actions—or *skills*—for solving long-horizon tasks is through constructing options [11]. An option  $o$  is described by a tuple  $(L_o, \pi_o, \beta_o)$ , where  $L_o$  denotes its initial condition,  $\pi_o$  is its closed-loop control policy, and  $\beta_o$  denotes the termination condition. However,  $\pi_o$  typically represents a single policy; to make execution more flexible, which is necessary for solving a category of similar tasks, the option should also be parameterized. In a parameterized skill [4], the policy  $\pi_o$  takes both a state and a continuous skill parameter  $z$  as input, and its behavior depends on  $z$ .

Sequential decision making problems with parameterized action space can be modeled as a parameterized action Markov Decision Process (PAMDP) [12], defined by the tuple  $\{S, H, T, R, \gamma\}$ , where the parameterized action space  $H$  can be defined as:  $H = \{(k, z_k) | z_k \in Z_k \text{ for all } k \in \{1, \dots, K\}\}$ , where  $Z_k$  is the corresponding continuous parameter set for each discrete action  $k \in \{1, \dots, K\}$ .  $z_k$  is the continuous parameter corresponding to  $k$ , and  $K$  is the total number of discrete actions. At each step, the agent must select both a discrete action  $k$  and a continuous parameter  $z_k$ . Thus, we have the dynamic transition function  $T(s'|s, k, z_k)$  and the reward function  $R(r|s, k, z_k)$ . A practical example is a soccer game, where the player needs to choose between kick the ball or move to some position (discrete), as well as the direction he wants to kick the ball to or the specific position  $(x, y, z)$  he wants to move to (continuous).

## 3 Meta-Learning Parameterized skills

In general, we want the agent to learn a set of parameterized skills suitable for use as the parameterized action space in a PAMDP, for which the agent will in turn learn a high-level control policy to solve new tasks. Following prior work [13], we use a discrete label to represent the skill type for one category of tasks. Then, the first question is how to learn the associated continuous parameters with this discrete action(label) that are able to **smoothly** cover policies with similar initial and terminal conditions but different behaviors. To this end, we focus on a parameterized skill learning setting, where the agent is given a set of tasks which share similar ultimate goals/reward functions but require diverse intermediate behaviors, as shown in Figure 2. We aim to learn a smooth parameterized representations of policies for such task set. Thus, by associating each discrete skill label with a continuous parameter, we enable them to be used in more situations where different parameters must be chosen, depending on the task context.

Formally, we model a parameterized skill as a Hidden Parameter MDP (HiP-MDP) [14], where a family of tasks is generated by varying a latent task parameter  $\omega$  drawn for each task according to  $P_\Omega$ . In Figure 2, the latent task parameter is the position of the doorway. Each setting of  $\omega$  specifies a unique MDP, but **the agent neither observes  $\omega$  nor has access to the function that generates the task family**. This is common in real-world scenarios, like we let the agent learn to drive different types of cars and then give it a new car. The difference between cars can be represented with some low-dimensional vector in principle but it would extremely hard to find that. The dynamics  $T(s'|s, a; \omega_i)$  and the reward function  $R(r|s, a; \omega_i)$  for task  $i$  depend on  $\omega_i \in \Omega$ , which is fixed for the duration of each specific task.

By modeling the parameterized skill as a HiP-MDP, the task set that we train our agent on has an underlying and potentially smoothly varying hidden parameter that controls the distinct features of each task like in Figure 2. Without showing this parameter to the agent, our goal then is to let the agent learn one single policy whose output behaviors are also controlled by a smoothly varying latent parameter.

Ideally, we want the agent to learn a policy that is able to solve the HiP-MDP, and also learn a continuous representation  $z$  that smoothly controls the behavior of the policy similar to how the hidden parameters  $\omega$  control the tasks' distinct features. A straightforward way then is to let the agent learn a skill conditioned policy that additionally takes the continuous representation  $z$  as a input, i.e.  $\pi : S \times Z \rightarrow A$ . Then, given different value of  $z$ , the policy will output actions that can solve different tasks. An existing framework that can help solve this problem is context-based meta-reinforcement learning (in particular, PEARL [5]). Each time when the agent must make a decision, a PEARL agent uses a context-encoder to map previously collected trajectories to a latent representation. The policy of PEARL is conditioned on both the current state and the latent representation. Originally, the context encoder is trained so that, when facing a new task, the agent only interacts with the environment for a few episodes and put the collected trajectories into the context encoder, then the agent can quickly infer which training task the new task is closer to and output the corresponding latent parameter to the policy. By contrast, in parameterized skill learning setting, besides the goal of learning a policy that performs well in all tasks, we also want that the continuous representation  $z$  which the policy is conditioned on is able to smoothly varying the agent's behaviors so that we can get a new smooth action space for this skill type and is reusable in other contexts.

We therefore adopt the context-based meta-RL framework in PEARL and train a context/trajectory encoder that aims to encode the collected trajectories into a latent representation, along with a actor and a critic network that both take in the latent representation as an additional input. In particular, the context encoder network  $\phi : \tau \rightarrow z$ , where the trajectory  $\tau = \{s_1, a_1, r_1, s_2, \dots, s_n\}$ . Then, the generated  $z$  can be viewed as part of the state and help the decision-making process by feeding into the actor network  $\pi(a|s, z)$  and critic network  $Q(s, a, z)$  as in PEARL. PEARL trained the context encoder in end-to-end fashion with loss from updating the critic network as well as an information bottleneck loss by computing KL divergence. We denote the combination of these two categories of loss as  $L_{\text{Value}}$ . In our case, besides working well on the given task set as a meta-RL algorithm, we also want the output latent representation of the context encoder to form a proper parameterized action space, so that we can easily reuse the learned skill-conditioned policy in other complicated tasks. To achieve this goal, we propose two additional trajectory-centric training objectives for the context encoder network. Note that instead of focusing on the difference between single transitions [15], we propose that parameterized skill learning should focus more on the overall difference between different trajectories, as shown in Figure 2. The learned representation of the skill should be able to encode the distinguishable features of the trajectories into its continuous parameters.

**Trajectory-Centric Diversity.** Skills with different continuous parameters should generate trajectories that can be discriminated from each other. As the skill-conditioned policy will be part of the environmental dynamics during second stage planning, diversity among the trajectories corresponding to different skills leads to less noise in the high level transitions (i.e., from one high-level state and a parameterized skill to the next high-level state, otherwise the uncertainty of this high-level dynamics

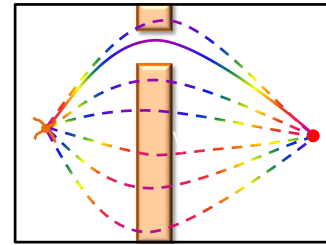


Figure 2: Parameterized skill learning: solving a parameterized family of tasks, with one behavior for each.

would be large), thus will accelerate learning. We seek to achieve this goal by gathering the latent representations of trajectories generated from the same task together in the latent representation space while pushing away others by minimizing InfoNCE loss [16]:

$$L_{\text{NCE}} := -\mathbb{E}[f(z_\mu, z_k) - \log \frac{1}{N} \sum_j \exp(f(z_\mu, z_j))],$$

where  $z_\mu$  and  $z_k$  are embeddings of trajectories sampled from the same task, and  $z_j$  are embeddings of trajectories from the other different tasks.  $N$  denotes the total number of sampled task at each training step, and  $f(\cdot)$  stands for the similarity score calculating function. More implementation details can be found in the appendix.

InfoNCE loss can be seen as an approximation of the mutual information between trajectories and their latent representation. Intuitively, by minimizing it, the trajectory encoder can generate latent representations by pulling together trajectories from the same tasks while pushing apart trajectories sampled from other tasks in the latent embedding space.

**Trajectory-Centric Smoothness.** As the new action space is synthesized from the learned skills, smoothness is required for this learned latent parameter space to be meaningful. We propose that the agent’s behavior under the skill-conditioned policy should change proportionally to the change of the continuous parameters’ value. We hope to implicitly encode the semantic meanings of the underlying hidden parameters into our latent skill representation, thus improve the smoothness of the latent skill embedding space. Therefore we add another learning objective that aims to embed intermediate features of the state trajectories into the latent representation. Our main intuition is that the distance of different skills in the latent space should be proportional to the distance between their trajectories. Specifically, suppose we sample two batches of trajectories  $\tau_1$  and  $\tau_2$  from two different tasks. Then, we write the smoothness term as:

$$L_{\text{Smoothness}} := \mathbb{E}_{\tau_1, \tau_2} [\|\phi(\tau_1) - \phi(\tau_2)\|_2 - \text{DTW}(\tau_1, \tau_2)],$$

where DTW stands for Dynamic Time Warping [17; 18]. Instead of directly computing the Euclidean distance between two state trajectories, we use Dynamic Time Warping to align the trajectories before measuring the distance. The idea is illustrated in Figure 3. Even from the exact same state and using the same policy, the pointwise Euclidean distance between two trajectories can be large as there exists uncertainty in both the environmental dynamics and the output actions from the policy. Thus, we use a more reasonable metric that compares the overall “shape” of the two trajectories, which is more consistent with our goal of extracting the overall features of the trajectory instead of focusing on specific transitions. By minimizing the smoothness term, we obtain skill embeddings that correspond to the dynamic time warping distance of trajectories.

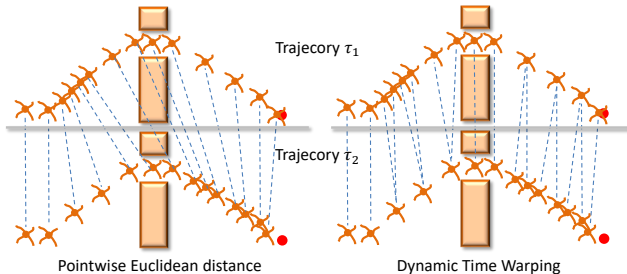


Figure 3: Trajectories’ Dynamic Time Warping distance compared with Pointwise Euclidean distance. Trajectory  $\tau_1$  and  $\tau_2$  are sampled from the task. Using Dynamic Time Warping to compute the distance (right) reveals they are quite close. However, unwarped pointwise Euclidean distance (left) ends up with the erroneous conclusion that the trajectories are very different.

**Parameterized Skill Learning (PSL) Objective.** Bringing these all together, we build a trajectory encoder network that maps trajectories from a specific task to a distribution of latent representations. The agent will then sample  $z$  from this distribution and feed it into the actor as well as critic network as an additional input to compute the actions as well as Q-values. The trajectory encoder  $\phi$  is trained end-to-end by minimizing a weighted sum of the value prediction, diversity, and smoothness losses:

$$L_{\text{Skill}} := L_{\text{Value}} + \alpha L_{\text{NCE}} + \beta L_{\text{Smoothness}},$$

where  $\alpha$  and  $\beta$  are hyperparameters that control the scale of each term. The training procedures of the other parts of the algorithm (including the structure of the skill-conditioned policy and value network) are the same as in PEARL. Full details can be found in the appendix. Note that we can discard the context encoder after the skill learning phase, as the agent will instead choose appropriate parameters when we reuse such skills in other tasks, which have different reward functions.

## 4 Learning with Learned Parameterized Actions

### 4.1 From MDP to Temporally-Extended PAMDP

As mentioned in previous section, a key motivation for learning parameterized skills is that it enables an agent to reuse those skills when learning to solve a new task.

Specifically, after we let the agent train on  $K$  different categories of tasks using PSL, we get  $K$  different skill-conditioned policies and fix them. Then we can directly let the high-level agent solve a new task by learning a policy that maps states to parameterized skill pairs  $(k, z_k)$ —learning in the high-level temporal-extended action space. Each discrete skill label corresponds to a low-level skill-conditioned policy network  $\pi_k(a|s, z_k)$ , which takes the continuous skill parameter  $z_k$  as an additional input. The decision making process of this new temporal-extended PAMDP is illustrated in Figure 4. Upon receiving a new observation, the agent must first choose the discrete skill label  $k$  using  $\pi_{\theta_d}$  and then choose the corresponding skill parameter  $z_k$  given the state  $s$  and  $k$  using  $\pi_{\theta_c}$ . The low-level skill-conditioned policy  $\pi_k(a|s, z_k)$ , which is learned by PSL and fixed, takes in the observation and the skill parameter and outputs a primitive action to interact with the environment. The discrete skill label and the continuous parameter are fixed and the low level policy  $\pi_k(a|s, z_k)$  will constantly output actions for a given number of environmental steps. Then, the last observation received from the environment is used as the new input state for the high-level policy, which will select new  $k$  and  $z_k$ , and so on. Note that in practice, we use information asymmetry similar to [19; 20]. That is, the observation received by the high-level policy contains more general information, like the position of the agent in the environment, while the observation received by the low level policy contains the proprioceptive state of the embodied agent, like the angle/velocity of different joints.

### 4.2 Hierarchical actor-critic with Parameterized Skills (HPS)

Then, the remaining question is how to efficiently learn a high-level control policy in this new abstracted PAMDP. Previous work has explored many methods to learn the parameterized/hybrid action space. In particular, HyAR [9] is a recently proposed algorithm that constructs a latent embedding space to model the dependency between discrete actions and continuous parameters. The latent embedding space is learned by training a conditional VAE [21] that learns to predict the next state given current state and parameterized actions. Then the discrete action along with the continuous parameters are mapped into a single latent action space, for which a policy is learned. However, learning directly in this latent embedding space means that the quality of exploration highly depends on whether the embedding space is learned properly. This problem becomes more severe as our parameterized action space are learned from data and can be quite noisy. That is, given the same state and the same parameterized skills, the distribution of the next state might have large uncertainty because executing each skill involves a large number of steps’ interaction with the environment, of which the resulting trajectories could be noisy even we add the diversity and smoothness constraint in last section. Thus, learning to embed this generated action space further into some latent space may magnify the uncertainty of transitions. Another straightforward but effective approach is P-DQN [10; 8]. The P-DQN agent maintains a separate policy network for each discrete action  $k$  to output the corresponding continuous parameters, and then feed all these parameters from different discrete actions into the critic network. This may induce high computational efficiency problem as it has to compute all the continuous parameters for each discrete action during both

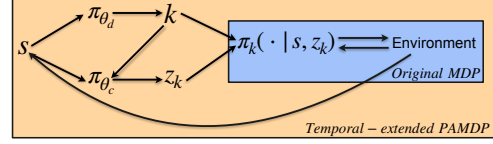


Figure 4: Decision making process in the temporally-extended PAMDP.  $\pi_{\theta_d}$  denotes the policy for discrete action and  $\pi_{\theta_c}$  denotes the policy for continuous parameters.

training and execution, and is magnified when the number of discrete actions are large. In our case, to enable structured exploration at both discrete action and continuous parameter level, we propose that to directly model the dependency of the discrete and continuous part of the parameterized action with two consecutive policy networks: for each decision-making step, we first choose the discrete action, then choose the continuous parameters conditioned on both the state and discrete action, which is in consistent with human’s decision making process [22].

Concretely, based on Figure 4, we decompose the policy of parameterized actions as:

$$\pi(k, z_k | s) = \pi_{\theta_c}(z_k | s, k) \pi_{\theta_d}(k | s),$$

where the policy network for discrete part of the action takes in state  $s$  and is parameterized by  $\theta_d$ , the policy network for the continuous parameter  $z_k$  takes in state and the discrete action  $k$  output from  $\pi_{\theta_d}$  and is parameterized by  $\theta_c$ . Compared with P-DQN, we only need to compute the continuous parameters for the discrete action we chose and thus avoid the redundancy problem.

We update the policy using actor-critic framework with the maximum entropy learning objective for reinforcement learning [23; 24]. Maximum entropy RL greatly improve the exploration especially in the face of estimation error. It functions by maximizing the entropy of the policy as well as the expected return. This particularly fits our framework as the parameterized action space is learned and can be quite noisy. Further, exploration with different rates at different time periods of training is important in the long-horizon tasks as we explained in introduction. Concretely, we update the critic network  $Q_{\psi}(s, k, z_k)$  according to:

$$L_{critic} = \mathbb{E}_{(s, k, z_k, r, s') \sim B} [Q_{\psi}(s, k, z_k) - (r + \gamma V(s))]^2,$$

where  $B$  denotes the replay buffer,  $V(s)$  denotes the value network. We update the policy (actor) networks according to:

$$L_{actor} = \mathbb{E}_{s \sim B, k \sim GS[\pi_{\theta_d}(s)]} \left[ D_{KL} \left( \pi_{\theta_c}(z_k | s, k) \middle\| \frac{\exp(Q_{\psi}(s, k, z_k))}{W_{\psi}(s)} \right) \right],$$

where  $W_{\psi}(s)$  is the partition function that normalizes the distribution,  $GS$  denotes the **gumbel-softmax** distribution [25]. That is, to enable structured exploration at different levels of the action execution phase, we use the maximum entropy training objective to augment exploration for the policy of continuous parameters  $\pi_{\theta_c}$ , while we use gumbel-softmax technique to sample the discrete action to further augment the exploration for the policy of discrete action  $\pi_{\theta_d}$ . Compared to  $\epsilon$ -greedy exploration strategy, gumbel-softmax further augments structured exploration by sampling from the categorical distribution. It enables computing gradients for parameters of  $\pi_{\theta_d}$ , of which the outputs are discrete, by leveraging the reparameterization trick [21]. We use gumbel-softmax to sample from the discrete policy network when interacting with the environment during training and also when updating the network. The latter one uses a smaller value of temperature  $\tau$  (controls the exploration rate) to make the updating process smoother following the intuition in [26].

Note that HHQN [27] which focuses on the parameterized action space problem in multi-agent domain also uses a similar consecutive policy networks structure. However, they use two different Q networks to approximate the value of discrete and continuous policy separately which may cause high-level non-stationary problem [9], i.e. when sampling a transition from the replay buffer during training, the same discrete action may not lead to the same reward and next state as the continuous parameter can be different from the moment it was chosen. Thus, computing the Q-value of a discrete action without considering the continuous parameter can be quite noisy. We avoid this problem as HPS has only one critic network that measures the value of the hybrid action pair as a whole.

## 5 Experiments

### 5.1 Parameterized Skill Learning

We first evaluate the performance of our parameterized skill learning algorithm on three different categories of tasks in the ant obstacle course domain. As shown in Figure 5, Ant-Goal requires the agent to walk past a doorway at a position unknown and unseen to the agent, and reach the goal on the other side. Ant-Bridge requires the agent to walk across a bridge with cross wind. The speed of the wind is unknown to the agent. Ant-Gather requires the agent to gather two coins along its way

to the goal position. The positions of the two coins are unknown to the agent. The agent succeeds after it reaches the goal position, which is fixed across all the tasks. The input states consist of the ant’s position (x-y-z coordinates) and other proprioceptive state, i.e., the angle/velocity of different joints. In these three tasks, the positions of the coins, the position of the doorway, and the wind speed are the corresponding hidden parameters in their MDPs, and the values of them are all sampled independently from a uniform distribution. The HiP-MDPs construct a standard meta-RL setting so we first compared with other meta-RL algorithms to see if the proposed trajectory-centric diversity and smoothness objectives in PSL can help the agent meta-training efficiently on a distribution of tasks. Specifically, we compared our algorithm PSL with PEARL [5], which is an off-policy context-based meta-RL algorithm on which PSL is based. We also compared to VariBAD [28], a recently proposed on-policy meta-RL algorithm, and another recurrence-based meta-RL method RL<sup>2</sup> [29]. We use the exact same evaluation (meta-testing) procedures as specified in PEARL.

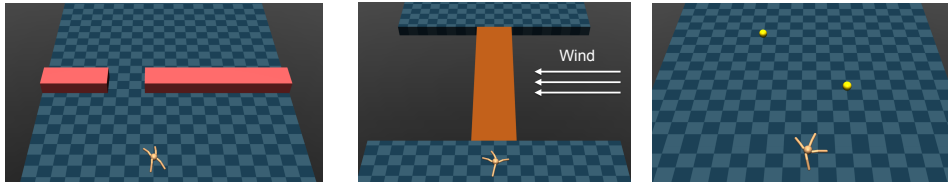


Figure 5: The environments we used for Parameterized skill learning experiments. From left to right: Ant-Goal, And-Bridge, Ant-Gather.

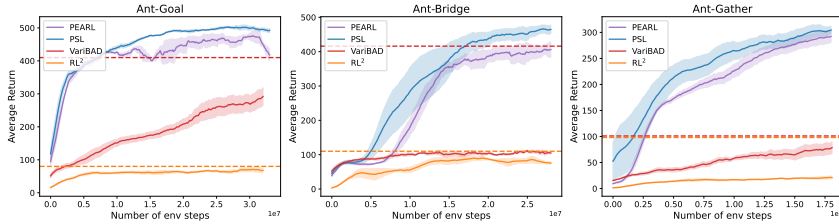


Figure 6: PSL’s performance when learning parameterized skills, as compared with other baselines. The plot shows average return on meta-test tasks v.s. the number of samples collected. Dashed lines correspond to the maximum return achieved by VariBAD and RL<sup>2</sup> after 1e8 environment steps.

The results of meta-testing performance are shown in Figure 6. PSL achieves better or comparable performance than the other baselines in all three tasks. Unlike the benchmark mujoco tasks in previous meta-RL papers, the difference between optimal policies in any one of these tasks are mainly from the trajectories as a whole, instead of the terminal states/goals. In such settings, which are common in practice, our proposed trajectory-centric diversity and smoothness objectives can help the agent encode the difference in trajectories into the latent embeddings, thus enabling the agent to quickly identify the correct embedding when adapting to a new task.

We then visualize the learned skill embeddings in four different domains. For each domain, We run the learned policies on 20 test tasks multiple times to collect trajectories. The test tasks are linearly sampled from the given task distribution. Then we encode the trajectories into latent embeddings using the trained context encoder. The original dimension of the latent skill is set to be 2 for all four domains so we just directly plot the latent embeddings in a 2-D space. As shown in Figure 7, the embeddings generated from the trajectories of the same tasks are close together in the latent space. Moreover, we can see a strong monotonic relationship between the components of the learned latent representation and the real position of the open space in Ant-goal, as well as the speed of the wind crossing the bridge. A similar conclusion can also be made in the Ant-gather-two-coins domain, where there are actually **two** variables for different tasks unlike the other three tasks, which only have one. We can see that the two dimensions of the latent skill approximate these two variables separately, showing a linear correlation between each coin’s position and the value of the latent representation. We also compared it with a visualization of the latent embedding encoded using PEARL’s context encoder. Without the proposed trajectory-centric diversity and smoothness objective, the learned skill embeddings have large areas of overlap and ignore important patterns in the trajectories influenced by the changing positions of the goals, except for Ant-Bridge.

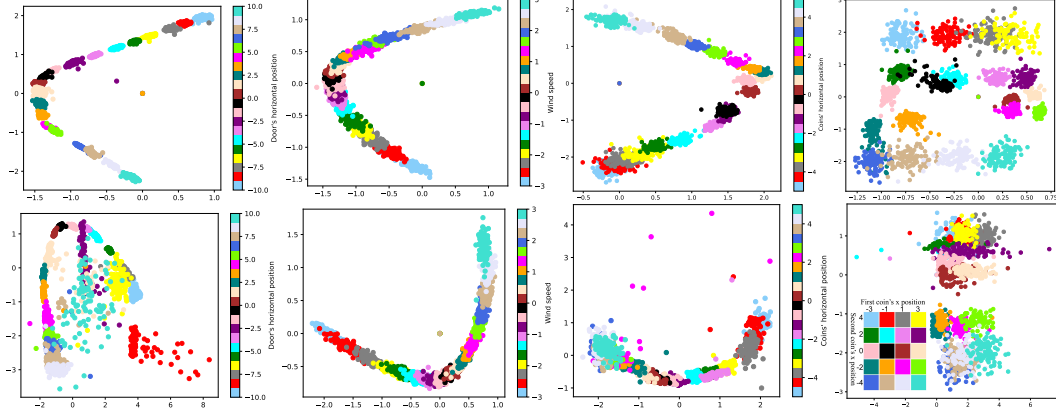


Figure 7: Visualization of learned skill embedding (best among three random seeds) of PSL (first row) and PEARL (second row), from left to right: Ant-Goal, Ant-Bridge, Ant-Gather-one-coin (only one coin’s position is changing), Ant-Gather-two-coins. We draw the ground-truth distribution of how the tasks are generated for ant-gather-two-coins at the bottom right corner of the last figure.

## 5.2 Learning with Learned Parameterized Skills

We then conducted experiments in the Ant obstacle course domain, shown in Figure 1. We consider two scenarios: 10 consecutive barriers sampled from 3 different categories of tasks introduced the previous section **(10b-3c)**, and 15 consecutive barriers sampled from 4 different categories of tasks **(15b-4c)**. The number of environment steps needed to complete the tasks and reach the final goal is around 3500 for 10b-3c, and around 5000 for 15b-4c. For each random seed of training, we sampled a sequence of 10/15 consecutive barriers as well as the hidden parameters of each barrier at the beginning of the experiment and fixed them for the rest of training and evaluation. We then used the parameterized skills learned in previous section as the new parameterized action space (i.e.  $\{Goal(x_1, x_2), Bridge(x_1, x_2), Gather(x_1, x_2), Box()\}$ ), and let HPS learn a solution policy for it. For the second scenario, we include Ant-push-box as a new task; the box’s position is fixed so we simply pretrain a SAC agent without skill parameters and add it to the skill set. The input states for HPS agent consist of only the ant’s absolute position in the environment, as well as an indicator of how many barriers the agent has passed. Note that these information are all independent of the subtask’s type and the hidden parameters of each subtask, which is not known to the agent. The low-level agent (pretrained skill-conditioned policies with PSL) takes in the ant’s position and proprioceptive state as input state which is consistent with the input when they were pretrained. We give the agent sparse staged reward: a positive reward is received only when the ant has passed a barrier or it reaches the final goal, otherwise, the reward is 0.

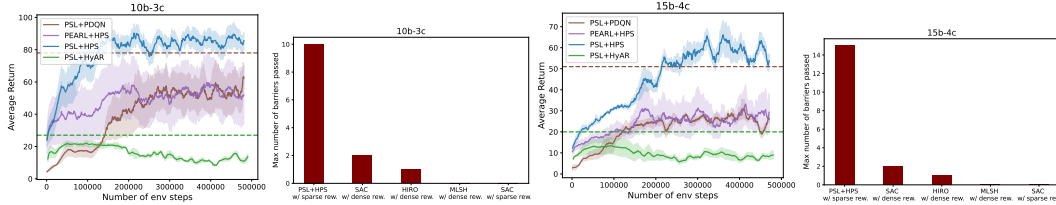


Figure 8: Comparison results of PSL + HPS against other baselines in both scenarios (10b-3c and 15b-4c). For the two plots, the horizontal axis denotes the number of “env” steps the **high-level** agent takes instead of the original environment steps, which is about 400× larger. Dashed lines correspond to the **maximum** return achieved by PSL+PDQN and PSL+HyAR after 1e6 “env” steps.

We compared to PEARL+HPS, which means that we run PEARL to learn the parameterized skills and use our proposed high-level planning algorithm HPS to learn the policy. We also compared to PSL+HyAR and PSL+PDQN, which means that we use the same parameterized skills learned by PSL but use different planning algorithm of parameterized action space to do high level planning. More-

over, we also compared to other algorithms that have the potential to perform well in long-horizon tasks: SAC [24]+dense reward, SAC+sparse reward, HIRO+dense reward [30], and MSLH+dense reward [31]. The dense reward used in these baselines are a composition of the exact same dense reward we use to pretrain the parameterized skills. The input states for these four baselines include all the information given to both levels of PSL+HPS agent.

As shown in Figure 8 and the attached video, the agent trained by our PSL+HPS algorithm is able to pass all 10/15 barriers, while the other algorithms even augmented with dense reward can pass two barriers at most. From the plots in Figure 8, we can see that the performance drops if we replace the parameterized skills learned by PSL with that of PEARNL. The performance gap is much larger than each single skill’s performance gap in 6, indicating that the proposed trajectory-centric diversity and smoothness learning objective help construct a better parameterized action space (7) which leads to better performance of high-level control policy. With the same pretrained parameterized skills, HPS learns the high-level control policy more efficiently than the other two PAMDP algorithms. PDQN reaches similar performance in the end but took twice as many environment steps compared to HPS due to the redundancy problem we explained in Section 4.2. HyAR fails to learn a good policy possibly because our parameterized action space is learned and synthesized so the noise of high level dynamics is magnified when planning in the further generated latent action space.

## 6 Related Work

Learning skills in a multi-task setting are common in prior work [32; 33; 34]. da Silva et al. [4] first propose to construct parameterized skills by analyzing the structure of policy manifold, but it needs labeled parameters of tasks for training and the approach can not be directly applied to complex problems. By contrast, we consider a HiP-MDP [14] setting where the task id/distinct information is not given to the agent in both skill learning and planning phases. This is the same setting as used in recent meta-RL works [35; 5] and is common in the real world. With the meta-RL setting, MSLH [31] learns fixed low-level policies during training and further finetune the high level policy on new tasks. Nam et al. [36] focus on using skilled pretrained from offline data to do better meta-RL. Some approaches also introduce multiple levels of hierarchies for skill learning [37] or planning [30]. Barreto et al. [38] and Qureshi et al. [39] propose a method to compose new task-relevant skills with pretrained simple skills. Goyal et al. [40] learn a high-level controller with decentralized low-level policies. However, these low-level skills are not parameterized so the generalization ability is limited. Rao et al. [19] introduce a similar three-level hierarchy of policies that also have discrete and continuous parts. However, they focus on learning skills from offline dataset and the learned skills do not involve temporal abstraction of the actions. Another category of skill learning method is unsupervised skill discovery [15; 41; 42], which is useful for exploring the environment before training and accelerating training on simple locomotion tasks. However, the pure unsupervised learning setting does not allow the agent to master one complete category of high-level skill, e.g., find the coffee machine in a house, because of lack of task-specific exploration as no environmental reward is given. Thus it’s hard to directly use these skills to solve long-horizon tasks.

A large body of recent work focuses on Deep RL problems with parameterized action space [12]. PADDPG [7] and HPPO [43] let the actor output an concatenation of the discrete action and the continuous parameters for each discrete action label together. This category of methods tends to ignore the dependency between discrete action and continuous parameter, which is crucial for finding the optimal parameterized action. P-DQN [10; 8] maintains a number of policy networks for each discrete action and its Q-network takes in the output continuous parameters from all possible discrete choices. Neunert et al. [44] also considers discrete-continuous control but the settings are not standard parameterized action space, i.e., the discrete part and the continuous part of action are independent of each other. HyAR [9] is a recent work that proposes to learn an action embedding of the parameterized action space and performs the best among the other baselines.

## 7 Conclusion

Motivated by the problems of solving long-horizon tasks, we propose to meta-learn transferable parameterized skills which can then be used as high-level actions in a new synthesized action space. We first propose two trajectory-centric training objectives for use in a context-based meta-RL framework, with the aim of synthesizing parameterized skills capable of expressing diverse

behaviors with a smooth parameter space. Then, we show how the original MDP is transformed into a temporal-extended PAMDP with the learning skills, and propose a new learning algorithm for the parameterized action space with simpler structures but exhibits better performance. Our empirical results demonstrate that our algorithm can learn transferable skills and efficiently solve complicated long-horizon continuous control tasks.

## References

- [1] John Schulman, Sergey Levine, Pieter Abbeel, Michael I. Jordan, and Philipp Moritz. Trust region policy optimization. In Francis R. Bach and David M. Blei, editors, *Proceedings of the 32nd International Conference on Machine Learning, ICML 2015, Lille, France, 6-11 July 2015*, volume 37 of *JMLR Workshop and Conference Proceedings*, pages 1889–1897. JMLR.org, 2015.
- [2] Timothy P. Lillicrap, Jonathan J. Hunt, Alexander Pritzel, Nicolas Manfred Otto Heess, Tom Erez, Yuval Tassa, David Silver, and Daan Wierstra. Continuous control with deep reinforcement learning. *CoRR*, abs/1509.02971, 2016.
- [3] Andrew G. Barto and Sridhar Mahadevan. Recent advances in hierarchical reinforcement learning. *Discrete Event Dynamic Systems*, 13:41–77, 2003.
- [4] Bruno Castro da Silva, George Dimitri Konidaris, and Andrew G. Barto. Learning parameterized skills. In *Proceedings of the 29th International Conference on Machine Learning, ICML 2012, Edinburgh, Scotland, UK, June 26 - July 1, 2012*. icml.cc / Omnipress, 2012.
- [5] Kate Rakelly, Aurick Zhou, Chelsea Finn, Sergey Levine, and Deirdre Quillen. Efficient off-policy meta-reinforcement learning via probabilistic context variables. In *Proceedings of the 36th International Conference on Machine Learning, ICML 2019*, volume 97 of *Proceedings of Machine Learning Research*, pages 5331–5340. PMLR, 2019.
- [6] Jane X. Wang, Zeb Kurth-Nelson, Dhruva Tirumala, Hubert Soyer, Joel Z. Leibo, Rémi Munos, Charles Blundell, Dharshan Kumaran, and Matthew Botvinick. Learning to reinforcement learn. *CoRR*, abs/1611.05763, 2016.
- [7] Matthew J. Hausknecht and Peter Stone. Deep reinforcement learning in parameterized action space. In Yoshua Bengio and Yann LeCun, editors, *4th International Conference on Learning Representations, ICLR 2016, San Juan, Puerto Rico, May 2-4, 2016, Conference Track Proceedings*, 2016.
- [8] Jiechao Xiong, Qing Wang, Zhuoran Yang, Peng Sun, Lei Han, Yang Zheng, Haobo Fu, T. Zhang, Ji Liu, and Han Liu. Parametrized deep q-networks learning: Reinforcement learning with discrete-continuous hybrid action space. *ArXiv*, abs/1810.06394, 2018.
- [9] Boyan Li, Hongyao Tang, Yan Zheng, Jianye Hao, Pengyi Li, Zhen Yu Wang, Zhaopeng Meng, and Li Wang. Hyar: Addressing discrete-continuous action reinforcement learning via hybrid action representation. *ArXiv*, abs/2109.05490, 2021.
- [10] Craig J. Bester, Steven James, and George Dimitri Konidaris. Multi-pass q-networks for deep reinforcement learning with parameterised action spaces. *ArXiv*, abs/1905.04388, 2019.
- [11] Richard S. Sutton, Doina Precup, and Satinder Singh. Between mdps and semi-mdps: A framework for temporal abstraction in reinforcement learning. *Artif. Intell.*, 112:181–211, 1999.
- [12] Warwick Masson, Pravesh Ranchod, and George Dimitri Konidaris. Reinforcement learning with parameterized actions. In Dale Schuurmans and Michael P. Wellman, editors, *AAAI, 2016*, pages 1934–1940, 2016.
- [13] Pierre-Luc Bacon, Jean Harb, and Doina Precup. The option-critic architecture. *ArXiv*, abs/1609.05140, 2017.
- [14] Finale Doshi-Velez and George Dimitri Konidaris. Hidden parameter markov decision processes: A semiparametric regression approach for discovering latent task parametrizations. *IJCAI : proceedings of the conference*, 2016:1432–1440, 2016.

- [15] Benjamin Eysenbach, Abhishek Gupta, Julian Ibarz, and Sergey Levine. Diversity is all you need: Learning skills without a reward function. In *7th International Conference on Learning Representations, ICLR 2019, New Orleans, LA, USA, May 6-9, 2019*, 2019.
- [16] Aäron van den Oord, Yazhe Li, and Oriol Vinyals. Representation learning with contrastive predictive coding. *CoRR*, abs/1807.03748, 2018.
- [17] Richard Bellman and Robert E. Kalaba. On adaptive control processes. *Ire Transactions on Automatic Control*, 4:1–9, 1959.
- [18] Meinard Müller. Dynamic time warping. In *Information retrieval for music and motion*, 2008.
- [19] Dushyant Rao, Fereshteh Sadeghi, Leonard Hasenclever, Markus Wulfmeier, Martina Zambelli, Giulia Vezzani, Dhruva Tirumala, Yusuf Aytar, Josh Merel, Nicolas Manfred Otto Heess, and Raia Hadsell. Learning transferable motor skills with hierarchical latent mixture policies. *ArXiv*, abs/2112.05062, 2021.
- [20] Josh Merel, Leonard Hasenclever, Alexandre Galashov, Arun Ahuja, Vu Pham, Greg Wayne, Yee Whye Teh, and Nicolas Manfred Otto Heess. Neural probabilistic motor primitives for humanoid control. *ArXiv*, abs/1811.11711, 2019.
- [21] Diederik P. Kingma and Max Welling. Auto-encoding variational bayes. *CoRR*, abs/1312.6114, 2014.
- [22] Thomas Parr and Karl J. Friston. The discrete and continuous brain: From decisions to movement—and back again. *Neural Computation*, 30:2319 – 2347, 2018.
- [23] Brian D. Ziebart, Andrew L. Maas, J. Andrew Bagnell, and Anind K. Dey. Maximum entropy inverse reinforcement learning. In *AAAI*, 2008.
- [24] Tuomas Haarnoja, Aurick Zhou, P. Abbeel, and Sergey Levine. Soft actor-critic: Off-policy maximum entropy deep reinforcement learning with a stochastic actor. In *ICML*, 2018.
- [25] Eric Jang, Shixiang Shane Gu, and Ben Poole. Categorical reparameterization with gumbel-softmax. *ArXiv*, abs/1611.01144, 2017.
- [26] Scott Fujimoto, Herke van Hoof, and David Meger. Addressing function approximation error in actor-critic methods. *ArXiv*, abs/1802.09477, 2018.
- [27] Haotian Fu, Hongyao Tang, Jianye Hao, Zihan Lei, Yingfeng Chen, and Changjie Fan. Deep multi-agent reinforcement learning with discrete-continuous hybrid action spaces. In *IJCAI*, 2019.
- [28] Luisa M. Zintgraf, Kyriacos Shiarlis, Maximilian Igl, Sebastian Schulze, Yarin Gal, Katja Hofmann, and Shimon Whiteson. Varibad: A very good method for bayes-adaptive deep rl via meta-learning. *ArXiv*, abs/1910.08348, 2020.
- [29] Yan Duan, John Schulman, Xi Chen, Peter L. Bartlett, Ilya Sutskever, and P. Abbeel. Rl2: Fast reinforcement learning via slow reinforcement learning. *ArXiv*, abs/1611.02779, 2016.
- [30] Ofir Nachum, Shixiang Shane Gu, Honglak Lee, and Sergey Levine. Data-efficient hierarchical reinforcement learning. In *NeurIPS*, 2018.
- [31] Kevin Frans, Jonathan Ho, Xi Chen, P. Abbeel, and John Schulman. Meta learning shared hierarchies. *ArXiv*, abs/1710.09767, 2018.
- [32] Nicolas Manfred Otto Heess, Greg Wayne, Yuval Tassa, Timothy P. Lillicrap, Martin A. Riedmiller, and David Silver. Learning and transfer of modulated locomotor controllers. *ArXiv*, abs/1610.05182, 2016.
- [33] Martin A. Riedmiller, Roland Hafner, Thomas Lampe, Michael Neunert, Jonas Degrave, Tom Van de Wiele, Volodymyr Mnih, Nicolas Manfred Otto Heess, and Jost Tobias Springenberg. Learning by playing - solving sparse reward tasks from scratch. *ArXiv*, abs/1802.10567, 2018.

[34] Karol Hausman, Jost Tobias Springenberg, Ziyun Wang, Nicolas Manfred Otto Heess, and Martin A. Riedmiller. Learning an embedding space for transferable robot skills. In *ICLR*, 2018.

[35] Chelsea Finn, P. Abbeel, and Sergey Levine. Model-agnostic meta-learning for fast adaptation of deep networks. In *ICML*, 2017.

[36] Taewook Nam, Shao-Hua Sun, Karl Pertsch, Sung Ju Hwang, and Joseph J. Lim. Skill-based meta-reinforcement learning. *ArXiv*, abs/2204.11828, 2022.

[37] John D. Co-Reyes, Yuxuan Liu, Abhishek Gupta, Benjamin Eysenbach, P. Abbeel, and Sergey Levine. Self-consistent trajectory autoencoder: Hierarchical reinforcement learning with trajectory embeddings. In *ICML*, 2018.

[38] André Barreto, Diana Borsa, Shaobo Hou, Gheorghe Comanici, Eser Aygün, Philippe Hamel, Daniel Toyama, Jonathan J. Hunt, Shibl Mourad, David Silver, and Doina Precup. The option keyboard: Combining skills in reinforcement learning. In *NeurIPS*, 2019.

[39] A. H. Qureshi, Jacob J. Johnson, Yuzhe Qin, Taylor Henderson, Byron Boots, and Michael C. Yip. Composing task-agnostic policies with deep reinforcement learning. In *ICLR*, 2020.

[40] Anirudh Goyal, Shagun Sodhani, Jonathan Binas, Xue Bin Peng, Sergey Levine, and Yoshua Bengio. Reinforcement learning with competitive ensembles of information-constrained primitives. *ArXiv*, abs/1906.10667, 2020.

[41] Archit Sharma, Shixiang Gu, Sergey Levine, Vikash Kumar, and Karol Hausman. Dynamics-aware unsupervised discovery of skills. In *8th International Conference on Learning Representations, ICLR 2020, Addis Ababa, Ethiopia, April 26-30, 2020*, 2020.

[42] Víctor Campos, Alexander Trott, Caiming Xiong, Richard Socher, Xavier Giro i Nieto, and Jordi Torres. Explore, discover and learn: Unsupervised discovery of state-covering skills. In *ICML*, 2020.

[43] Zhou Fan, Rui long Su, Weinan Zhang, and Yong Yu. Hybrid actor-critic reinforcement learning in parameterized action space. In *IJCAI*, 2019.

[44] Michael Neunert, Abbas Abdolmaleki, Markus Wulfmeier, Thomas Lampe, Jost Tobias Springenberg, Roland Hafner, Francesco Romano, Jonas Buchli, Nicolas Manfred Otto Heess, and Martin A. Riedmiller. Continuous-discrete reinforcement learning for hybrid control in robotics. *ArXiv*, abs/2001.00449, 2019.

[45] Michael Laskin, Aravind Srinivas, and Pieter Abbeel. CURL: contrastive unsupervised representations for reinforcement learning. In *Proceedings of the 37th International Conference on Machine Learning, ICML 2020, 13-18 July 2020, Virtual Event*, volume 119 of *Proceedings of Machine Learning Research*, pages 5639–5650. PMLR, 2020.

[46] Haotian Fu, Hongyao Tang, Jianye Hao, Chen Chen, Xidong Feng, Dong Li, and Wulong Liu. Towards effective context for meta-reinforcement learning: an approach based on contrastive learning. In *Thirty-Fifth AAAI Conference on Artificial Intelligence, AAAI 2021, 2021*, pages 7457–7465. AAAI Press, 2021.

[47] Nikhil Mishra, Mostafa Rohaninejad, Xi Chen, and Pieter Abbeel. A simple neural attentive meta-learner. In *6th International Conference on Learning Representations, ICLR 2018, Vancouver, BC, Canada, April 30 - May 3, 2018, Conference Track Proceedings*. OpenReview.net, 2018.

[48] Greg Brockman, Vicki Cheung, Ludwig Pettersson, Jonas Schneider, John Schulman, Jie Tang, and Wojciech Zaremba. Openai gym. *CoRR*, abs/1606.01540, 2016.

[49] Emanuel Todorov, Tom Erez, and Yuval Tassa. Mujoco: A physics engine for model-based control. In *2012 IEEE/RSJ International Conference on Intelligent Robots and Systems, IROS 2012, Vilamoura, Algarve, Portugal, October 7-12, 2012*, pages 5026–5033. IEEE, 2012.

## A Appendix

### A.1 Parameterized Skill Learning (PSL) Algorithm

---

**Algorithm 1** Parameterized Skill Learning (PSL) Meta-training (regular encoder network)

---

**Input:** Batch of training tasks  $\mu_{i=1, \dots, M}$  from  $p(\mu)$ ,  
 Initialize replay buffer  $B_i$  for each training task  
 Initialize parameters  $\theta_a$  and  $\theta_c$  for the actor and critic networks separately.  
 Initialize parameters context encoder network  $\phi$ , context encoder target network  $\phi_{target}$

**while** not done **do**

**for** each task  $\mu_i$  **do**

Roll out policy  $\pi_{\theta_a}$ , producing transitions  $\{(s_j, a_j, r_j, s'_j)\}_{j:1 \dots N}$

Add tuples to execution replay buffer  $B_i$

**end for**

**if** there's at least one success trajectory in each task's replay buffer **then**

$calculating\_DTW = True$

**end if**

**for** each training step **do**

Sample a meta batch of tasks  $\{1, \dots, C\}$

**for** each task  $i$  in meta batch **do**

Sample two transition batches  $b_1^i = \{(s_k, a_k, r_k, s'_k)\}_{k=1 \dots K} \sim B_i$ ,  $b_2^i = \{(s_k, a_k, r_k, s'_k)\}_{k=1 \dots K} \sim B_i$

Sample latent embedding  $z_1^i \sim \phi(b_1^i)$ ,  $z_{target}^i \sim \phi_{target}(b_2^i)$

Update actor and critic networks with  $\{z_1^i, b_1^i\}$ , and calculate  $L_{Value}$

**end for**

Calculate InfoNCE loss  $L_{NCE}$  with  $\{z_1^1, \dots, z_1^C\}$ ,  $\{z_{target}^1, \dots, z_{target}^C\}$

**if**  $calculating\_DTW = True$  **then**

Sample one success trajectory from each task's replay buffer:  $\{\tau_{suc}^1, \dots, \tau_{suc}^C\}$

Calculate Dynamic Time Warping loss  $L_{Smoothness}$  with  $\{z_1^1, \dots, z_1^C\}$ ,  $\{z_{target}^1, \dots, z_{target}^C\}$ ,  $\{\tau_{suc}^1, \dots, \tau_{suc}^C\}$

**end if**

Update context encoder network with  $L_{Skill} = L_{Value} + \alpha L_{NCE} + \beta L_{Smoothness}$

**end for**

**end while**

---

We show detailed procedures in Algorithm 1. The training procedures for the actor and critic networks are the same as in PEARL. After collecting data, for each training step, we first sample a meta batch of tasks  $\{1, \dots, C\}$ . Then for each task, we sample two transition batches  $b_1^i$  and  $b_2^i$  from its own replay buffer. We feed the first transition batch into the context encoder, then use the output latent embedding to calculate the RL loss  $L_{Value}$  and update actor and critic network parameters. This procedure is the same as in PEARL. We feed the second transition batch into the target context encoder network to get the latent embedding which will be used to calculate the auxiliary losses. After we get all the latent embeddings for tasks in the meta batch, we first calculate the InfoNCE loss using the latent embedding pairs from given task set. Then, if each task has collected at least one success trajectory (that is, the agent successfully reached the goal position), we will let the agent also calculate Dynamic Time Warping loss with the latent embedding and success trajectories sampled for each task in the meta batch. And we will update the context encoder network's parameters at the end of this training step. Note that one limitation of the implementation here is that for some tasks, it is possible that not all tasks in the training task set can collect a success trajectory within the given number of episodes. This will lead to the problem that the DTW is not calculated and used throughout the training process. Thus, we provide another implementation in A.1.2, which does not have such requirement and achieves similar final performance.

For calculating InfoNCE loss, we adopt the same procedures in [45; 46], where we model the similarity score calculating function as bilinear products, i.e.  $z_\mu^T W z_k$ , where  $W$  is the learned

parameter. Using the denotations in Algorithm 1, for  $z_1^1$ , we can rewrite the InfoNCE loss as:

$$L_{\text{NCE}} := -\mathbb{E}[f(z_1^1, z_{\text{target}}^1) - \log \frac{1}{N} \sum_{j=2}^C \exp(f(z_1^1, z_{\text{target}}^j))].$$

And we calculate the loss use same procedures for other latent embedding  $\{z_1^2, \dots, z_1^C\}$ .

For calculating Dynamic Time Warping loss, given a latent embedding pair from different tasks:  $(z_1^j, z_{\text{target}}^k)$ , we draw the corresponding pair from the success trajectories set:  $(\tau_{\text{suc}}^j, \tau_{\text{suc}}^k)$ , and calculate the DTW loss with:

$$L_{\text{Smoothness}} := \mathbb{E}_{\tau_{\text{suc}}^j, \tau_{\text{suc}}^k} [|z_1^j - z_{\text{target}}^k|_2 - \kappa \text{DTW}(\tau_{\text{suc}}^j, \tau_{\text{suc}}^k)], \quad (1)$$

where  $\kappa$  denotes the hyperparameter controls the scale of the DTW distance.

Different from standard meta-RL setting, we assume the training task set (a fixed number of tasks) is given, whereas in [35] each time a task is randomly generated using parameters sampled from a prior distribution.

Table 1: PSL’s hyperparameters

Environment	# Meta-train tasks	$\alpha$	$\beta$	$\kappa$	Meta batch size	Embedding batch size
Ant-goal	100	10	1	0.5	16	100
Ant-bridge	100	100	1	0.1	16	50
Ant-gather-one-coin	100	10	1	0.5	16	100
Ant-gather-two-coins	200	10	0.1	0.5	32	150

### A.1.1 Implementation details

When computing the latent embedding  $z$  using context encoder, the state component in the input trajectory only contains the first two elements (x&y coordinates of the ant) for ant-goal and ant-gather, for ant-bridge the state component in the input trajectory is the original state. Both actor network and critic network in PSL are parameterized MLPs with 2 hidden layers of (300, 300) units. The context/trajectory encoder network is modeled as product of independent Gaussian factors, with 3 hidden layers of (400, 400, 400) units. We set the learning rate as  $3e-4$ . The scale of KL divergence loss is set to be 0.1. Other hyperparameters are listed in Table 1.

### A.1.2 Another approach for implementing the context encoder and its training process

Based on the intuition that the distance of different skills in the latent space should be proportional to the distance between their trajectories, we can compute DTW distance for any pair of trajectories, no matter if they succeed or not, and match the distance to their corresponding latent embeddings’ distance. Thus, we do not need to wait until there’s at least one success trajectory in each task’s replay buffer to calculate the smoothness loss.

Concretely, we provide the algorithm in Algorithm 2. Instead of modeling the context/trajectory encoder network as a product of independent Gaussian factors, we use a sequential encoder network, SNAIL [47], which uses temporal convolution and soft attention. Then, at each training step, instead of sampling two random batches of **transitions**, we sample two complete **trajectories**  $\tau_1, \tau_2$  and transform them to the same length. We compute the corresponding latent embeddings  $z_1, z_2$  for both of them using the context encoder, and calculate the DTW distance as well as the smoothness loss using the same equation (1). Thus we update the encoder network with the smoothness loss at every training step.

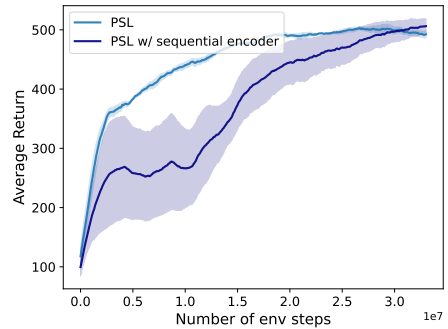


Figure 9: Comparison of different implementation strategy for PSL on Ant-goal.

We show the results comparison in Figure 9. Although PSL with sequential encoder does not learn as fast as the original version, it achieves similar final performance. Besides, the requirement for using this version of the algorithm is a little looser. The readers can choose to apply one of the two versions of our algorithm based on the properties of their own test tasks.

---

**Algorithm 2** Parameterized Skill Learning (PSL) Meta-training (Sequential encoder network)

---

**Input:** Batch of training tasks  $\mu_{i=1,\dots,M}$  from  $p(\mu)$ ,  
 Initialize replay buffer  $B_i$  for each training task  
 Initialize parameters  $\theta_a$  and  $\theta_c$  for the actor and critic networks separately.  
 Initialize parameters context encoder network  $\phi$ , context encoder target network  $\phi_{target}$

**while** not done **do**

- for** each task  $\mu_i$  **do**
- Roll out policy  $\pi_{\theta_a}$ , producing transitions  $\{(s_j, a_j, r_j, s'_j)\}_{j:1\dots N}$
- Add tuples to execution replay buffer  $B_i$
- end for**
- if** there's at least one success trajectory in each task's replay buffer **then**
- $calculating\_DTW = True$
- end if**
- for** each training step **do**
- Sample a meta batch of tasks  $\{1, \dots, C\}$
- for** each task  $i$  in meta batch **do**
- Sample two trajectories and transform them to same length  $K$ :  $\tau_1^i = \{(s_k, a_k, r_k, s'_k)\}_{k=1\dots K} \sim B_i$ ,  $\tau_2^i = \{(s_k, a_k, r_k, s'_k)\}_{k=1\dots K} \sim B_i$
- Sample latent embedding  $z_1^i \sim \phi(\tau_1^i)$ ,  $z_{target}^i \sim \phi_{target}(\tau_2^i)$
- Sample transition batch  $b^i = \{(s_k, a_k, r_k, s'_k)\}_{k=1\dots K} \sim B_i$
- Update actor and critic networks with  $\{z_1^i, b^i\}$ , and calculate  $L_{Value}$
- end for**
- Calculate InfoNCE loss  $L_{NCE}$  with  $\{z_1^1, \dots, z_1^C\}$ ,  $\{z_{target}^1, \dots, z_{target}^C\}$
- Calculate Dynamic Time Warping distance and Smoothness loss  $L_{Smoothness}$  with  $\{z_1^1, \dots, z_1^C\}$ ,  $\{z_{target}^1, \dots, z_{target}^C\}$ ,  $\{\tau_1^1, \dots, \tau_1^C\}$ ,  $\{\tau_2^1, \dots, \tau_2^C\}$
- Update cotext encoder network with  $L_{Skill} = L_{Value} + \alpha L_{NCE} + \beta L_{Smoothness}$
- end for**

**end while**

---

## A.2 Hierarchical actor-critic with Parameterized Skills (HPS)

### A.2.1 Further Comparison with other existing RL with parameterized action space algorithms

We show a comparison of different algorithms' properties in Table 2. P-DQN lacks scalability as it maintains a separate actor network for each discrete action, and have to compute all of them during both training and execution as we explained in the main text. HHQN has the problem of potential nonstationarity as we explained in the last paragraph of Section 4.2. PADDPG makes the actor output an concatenation of the discrete action and the continuous parameters for each of them together, which tends to ignore the dependency between discrete action and continuous parameters. This leads to performance drop as shown in PDQN and HyAR's original papers. HyAR don't have the above three problems but it needs to further learn a latent action space and plan based on it instead of the primitive parameterized action space. In our scenario where the parameterized action space is actually learned, the noise in the dynamics is magnified and it's hard to learn a proper latent action space. We assume this leads to HyAR's performance drop in our experiments.

### A.2.2 Implementation details

For the actor of discrete action  $\pi_{\theta_d}$ , we use two hidden layers of MLPs with (300, 300) units, the output layer follows by a gumbel-softmax layer. For both the actor of continuous parameters  $\pi_{\theta_c}$  and critic network, we use two hidden layers of MLPs with (300, 300) units. The learning rates are all set as  $3e - 4$ . The output of the actor of continuous parameters are stochastic the same as in SAC. Note that we fix the temperature for gumbel-softmax to be 1.0 across the whole training process, without

Table 2: Comparison with other parameterized action space algorithms

Algorithm	Scalability	Stationarity	Dependence	Primitive
P-DQN	✗	✓	✓	✓
PADDPG	✓	✓	✗	✓
HHQN	✓	✗	✓	✓
HyAR	✓	✓	✓	✗
HPS	✓	✓	✓	✓

using any decaying strategy. We also tried automatic temperature tuning as in SAC but did not get satisfactory result. We set the reward scale as 5 and the batch size as 128.

### A.3 Environment details and baselines

We run all experiment with OpenAI gym [48], with the mujoco simulator [49]:

- Ant-goal: The horizontal position of the doorway changes across all the tasks (uniformly sampled from  $[-10, 10]$ ). The other environmental properties are fixed, including the goal’s position. The task horizon is 400. The agent succeeds when it reaches the goal position ( $x = 0, y = 25$ ). The state input includes the position and velocity of different joints of ant, and the ant’s horizontal position  $x$ , as well as its relative vertical position  $y$  to the midlane  $y = 10$ .
- Ant-bridge: The wind speed when the ant is on the bridge changes across all the tasks (uniformly sampled from  $[-3, 3]$ ). The other environmental properties are fixed. The task horizon is 300. The agent succeeds when it reaches the goal position ( $x = 0, y = 26$ ). The state input includes the position and velocity of different joints of ant, and the ant’s horizontal position  $x$ , as well as its relative vertical position  $y$  to the midlane  $y = 10$ .
- Ant-gather: The position of the first coin (Ant-gather-one-coin) or both coins (Ant-gather-two-coins) change across all the tasks (uniformly sampled from  $[-4.5, 4.5]$ ). The other environmental properties are fixed<sup>2</sup>. The task horizon is 400. The agent succeeds only when it gathers both coins and reaches the goal position ( $x = 0, y = 16$ ). The state input includes the position and velocity of different joints of ant, an indicator for how many coins the ant has gathered, and the ant’s horizontal position  $x$ , as well as its relative vertical position  $y$  to the midlane  $y = 8$ .
- Ant-box: The ant needs to push the box and walk pass a gap to reach the goal position. The position of the box is fixed. The task horizon is 500.
- Ant-mix: The ant needs pass 10/15 different barriers consist of Ant-goal, Ant-bridge, Ant-gather-one-coin, Ant-box and reach the goal position. The task order as well as their specific features (door position, wind speed etc.) are all fixed. The original task horizon is 4000/6000. The task horizon when we do high-level learning with the skills is 10/15. The state input includes: High-level: the ant’s horizontal position  $x$  and vertical position  $y$ , how many barrier it has passed. Low-level: the ant’s horizontal position  $x$  and its relative vertical position  $y$  to the midlane of the current subtask, as well as the position and velocity of different joints of ant, and how many coins the ant has gathered.

Reward Functions:

- Ant-goal:

$$R_t = \mathbb{I}\{\text{The ant has not passed the door}\} * \Delta d_{\text{Distance to door}} + \mathbb{I}\{\text{door}\} * 10 \\ + \mathbb{I}\{\text{The ant has passed the door}\} * \Delta d_{\text{Distance to goal}} + \mathbb{I}\{\text{goal}\} * 20$$

- Ant-bridge:

$$R_t = \Delta d_{\text{Distance to goal}} + \mathbb{I}\{\text{goal}\} * 20$$

<sup>2</sup>Note that in this paper, we consider the HiP-MDP setting. If we change the task order as well as the task parameters, without giving the agent these information the problem would become partially observable and extremely hard to solve.

- Ant-gather:

$$\begin{aligned}
R_t = & \mathbb{I}\{\text{The ant has not gathered the first coin}\} * \Delta d_{\text{Distance to first coin}} + \mathbb{I}\{\text{first coin}\} * 10 \\
& + \mathbb{I}\{\text{The ant has gathered one coin, one left}\} * \Delta d_{\text{Distance to second coin}} + \mathbb{I}\{\text{second coin}\} * 10 \\
& \mathbb{I}\{\text{The ant has gathered two coins}\} * \Delta d_{\text{Distance to goal}} + \mathbb{I}\{\text{goal}\} * 20
\end{aligned}$$

- Ant-mix (sparse):

$$R_t = \mathbb{I}\{\text{The ant passed a barrier}\} * 5 + \mathbb{I}\{\text{goal}\} * 100$$

- Ant-mix (dense): For the dense reward used by other baselines, we use the direct combination of the dense reward we set for each specific subtask. The environment knows what the subtask is and it will give the corresponding dense reward. Moreover, we also give it the sparse reward when it passes each barrier.

The results shown in the main text are averaged over three random seeds. The error bar shows one standard deviation. All experiments were run on our university’s high performance computing cluster. When comparing with PDQN & HyAR & PEARL in ant obstacle course (ant-mix) domain (results shown in two plots of Figure 8), we fix the task order across different random seeds to make the environment setting consistent to all baselines. For comparison with HIRO & SAC & MLSH, we let all methods try 5 different task orders and task parameter (hidden parameter) pairs.

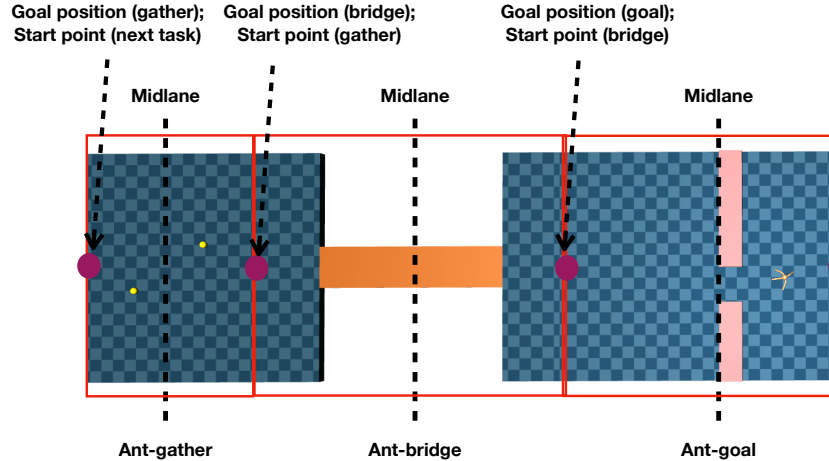


Figure 10: Ant obstacle course (ant-mix) further illustration.

Baselines: 1. Parameterized skill learning: We use the original source code for PEARL<sup>3</sup>, VariBAD<sup>4</sup> and their implementation for RL<sup>2</sup>. 2. Learning with learned parameterized skills: We use the original code for HyAR-TD3<sup>5</sup>, and their implementation for PDQN-TD3. We also use the original code for MLSH<sup>6</sup> and HIRO<sup>7</sup>. For SAC, we use the stable-baselines3 implementation<sup>8</sup>. Additionally, for HyAR, we let the agent pretrain the Variational Auto-encoder 2000 steps. For MLSH, the subtask order is fixed during training, but we let the agent randomly placed at one of the start points (see Figure 10) at the beginning of each episode.

#### A.4 More Experimental results

We compared the difference between DTW distance and pointwise euclidean distance. For each domain (ant-goal, ant-bridge, ant-gather), we test two scenarios: **same tasks**, where we fix the hidden

<sup>3</sup><https://github.com/katerakelly/oyster>

<sup>4</sup><https://github.com/lmzintgraf/varibad>

<sup>5</sup>[https://github.com/TJU-DRL-LAB/AI-Optimizer/tree/1e2a33a4a3a7a8235f1c12ea71b1ea686c071094/self-supervised-r1/RL\\_with\\_Action\\_Representation/HyAR](https://github.com/TJU-DRL-LAB/AI-Optimizer/tree/1e2a33a4a3a7a8235f1c12ea71b1ea686c071094/self-supervised-r1/RL_with_Action_Representation/HyAR)

<sup>6</sup><https://github.com/openai/mlsh>

<sup>7</sup>[https://github.com/watakandai/hiro\\_pytorch](https://github.com/watakandai/hiro_pytorch)

<sup>8</sup><https://github.com/DLR-RM/stable-baselines3>

parameter (door position/wind speed/coin position), and calculate the distance between success trajectories that are able to solve the same task. Another scenario is **neighbour tasks**, where we sample 5 values from the original range of the hidden parameter with same distance from each other. For instance, for ant-goal, we sample 5 doorway position:  $\{-9, -4.5, 0, 4.5, 9\}$ . Then we calculate the distance between success trajectories from two neighbour tasks. Ideally, the distance of different pairs of neighbour tasks (e.g.  $\{-9, -4.5\}$  &  $\{-4.5, 0\}$ ) should be similar to each other, as the actual distance between the hidden parameters are the same.

We show the Coefficient of Variation of the two methods for calculating distance in different scenarios in Figure 11. In both same tasks and neighbour tasks scenarios, we expect the coefficient of variation to be small. This is because different metrics will result in different means, but the variation of the distance should be small as these distance are either calculated for the same tasks (that is, actual hidden parameter distance is fixed as 0) or for tasks with the same actual hidden parameter distance. We find that the distance calculated by DTW gets smaller variation in all scenarios which is consistent to our hypothesis. The gap between the two methods is especially large for trajectories from the same tasks, indicating that unwrapped pointwise Euclidean distance can end up with the erroneous conclusion that the trajectories are very different even though they have quite similar overall shape.

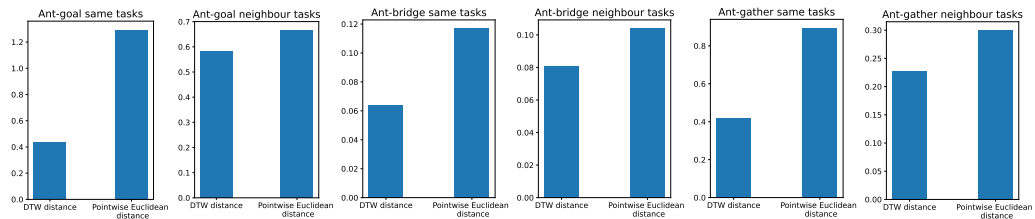


Figure 11: Comparison results of DTW distance against pointwise euclidean distance in **Coefficient of Variation**. In all scenarios, we collect ten pairs of data (two categories of distance) and then compute the coefficient of variation for the ten values.

We also compare the metrics for calculating the distance between  $z$  when calculating the DTW distance, shown in Figure 12 Left. We find that besides directly using Euclidean distance as in Equation (1), we can also use the similarity score function  $f$  to calculate the distance between two latent embedding. And the result shows that these two metrics achieve similar results, although the performance of using similarity score drops a bit at the end of training. As shown in Figure 12 Right, compared with regular epsilon-greedy strategy, our exploration strategy based on gumbel-softmax is important for HPS to achieve good performance on ant obstacle course tasks. Moreover, we do not need to consider the additional hyperparameters brought by epsilon-greedy method (final epsilon, number of decay steps) and just fix the “temperture” of gumbel-softmax to be 1.0 for all the scenarios.

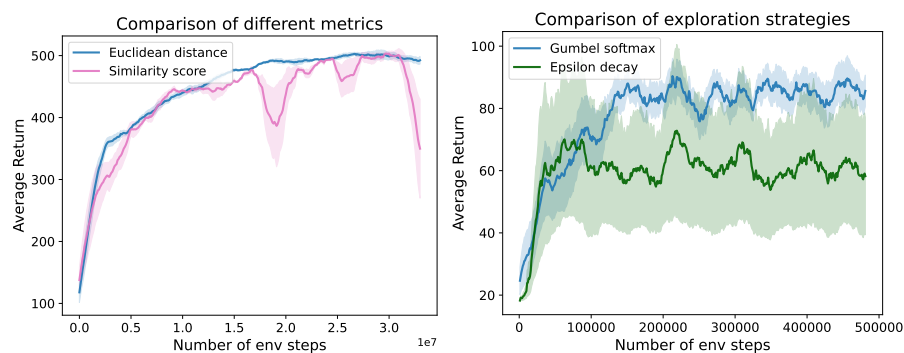


Figure 12: Left: Comparison of different metrics for calculating the distance between latent embeddings on Ant-goal. Right: Comparison of different exploration strategies for *HPS* on Ant obstacle course 10b-3c.